Cell-to-Cell Measles Virus Spread between Human Neurons Is Dependent on Hemagglutinin and Hyperfusogenic Fusion Protein

佐藤, 裕真

Cell-to-cell measles virus spread between human neurons dependent on the hemagglutinin and the hyperfusogenic fusion protein

Yuma Sato[1], Shumpei Watanabe[1,2], Yoshinari Fukuda[1], Takao Hashiguchi[1], Yusuke Yanagi[1#], Shinji Ohno[1,3#]

[1]Department of Virology, Faculty of Medicine, Kyushu University, Fukuoka, Japan

[2]Special Pathogens Laboratory, Department of Virology I, National Institute of Infectious Diseases, Tokyo, Japan

[3]Department of Virology, Graduate School of Medicine, University of the Ryukyus, Okinawa, Japan

Running Title: Measles virus spread between human neurons

Address Correspondence to

Yusuke Yanagi, yyanagi@virology.med.kyushu-u.ac.jp or

Shinji Ohno, soono@med.u-ryukyu.ac.jp

Abstract: 247 words

Importance: 146 words

Text: 3916 words

Abstract

Measles virus (MV) usually causes acute infection, but in rare cases persists in the brain, resulting in subacute sclerosing panencephalitis (SSPE). Since human neurons, an important target affected in the disease, do not express the known MV receptors (signaling lymphocyte activation molecule (SLAM) and nectin 4), how MV infects neurons and spreads between them is unknown. Recent studies have shown that many virus strains isolated from SSPE patients possess substitutions in the extracellular domain of the fusion (F) protein which confer enhanced fusion activity. Hyperfusogenic viruses with such mutations, unlike the wild-type MV, can induce cell-cell fusion even in SLAM- and nectin 4-negative cells and spread efficiently in human primary neurons and the brains of animal models. We here show that a hyperfusogenic mutant MV (IC323-F(T461I)-EGFP), but not the wild-type MV, spreads in differentiated NT2 cells, a widely-used human neuron model. Confocal time-lapse imaging revealed the cell-to-cell spread of IC323-F(T461I)-EGFP between NT2 neurons without syncytium formation. The production of virus particles was strongly suppressed in NT2 neurons, also supporting the cell-to-cell viral transmission.

52 The spread of IC323-F(T461I)-EGFP was inhibited by the fusion inhibitor
53 peptide as well as by some but not all of anti-hemagglutinin antibodies which
54 neutralize SLAM- or nectin-4-dependent MV infection, suggesting the presence
55 of a distinct neuronal receptor. Our results indicate that MV spreads in a
56 cell-to-cell manner between human neurons without causing syncytium
57 formation, and that the spread is dependent on the hyperfusogenic F protein,
58 the hemagglutinin and the putative neuronal receptor for MV.
59
60 **Importance**
61 Measles virus (MV), in rare cases, persists in the human central nervous system
62 (CNS) and causes subacute sclerosing panencephalitis (SSPE) several years
63 after acute infection. This neurological complication is almost always fatal, and
64 there is currently no effective treatment for it. Mechanisms by which MV
65 invades the CNS and causes the disease remain to be elucidated. We have
66 previously shown that fusion-enhancing substitutions in the fusion protein of
67 MVs isolated from SSPE patients contribute to MV spread in neurons. In this
68 study, we demonstrate that MV bearing the hyperfusogenic mutant fusion

protein spreads between human neurons in a cell-to-cell manner. Spread of the virus was inhibited by the fusion inhibitor peptide and antibodies against the MV hemagglutinin, indicating that both the hemagglutinin and hyperfusogenic fusion protein play important roles in MV spread between human neurons. The findings help us better understand the disease process of SSPE.

Introduction

Measles, characterized by high fever, conjunctivitis and a maculopapular rash, is caused by measles virus (MV), a highly contagious human pathogen (1). Effective live vaccines have greatly reduced its morbidity and mortality, but measles is still prevalent in certain developing countries (2). MV rarely establishes persistent infection in the central nervous system (CNS), and several years after acute infection, 6.5 to 11 cases per 100,000 cases of measles develop subacute sclerosing panencephalitis (SSPE) (3) and the risk of developing SSPE is much higher for children contracting measles infection below 5 years of age (4). Patients with SSPE exhibit characteristic clinical manifestations such as personality changes, myoclonus and dementia, and

there is currently no effective treatment for the disease (5).

MV is a member of the genus *Morbillivirus* of the family *Paramyxoviridae*, and possesses a non-segmented, negative-sense RNA genome with 6 genes encoding the nucleocapsid (N), phospho- (P), matrix (M), fusion (F), hemagglutinin (H), and large (L) proteins, respectively (1). The P gene also encodes non-structural proteins V and C. The N protein encapsidates the viral genome, forming the nucleocapsid, which is bound by the RNA-dependent RNA polymerase comprised of the L and P proteins. This ribonucleoprotein (RNP) complex binds to the M protein, which interacts with cytoplasmic tails of the H and F proteins and is responsible for the assembly of virus particles. The H and F proteins are envelope glycoproteins, and mediate receptor binding and membrane fusion, respectively. Binding of the H protein to a cellular receptor induces conformational changes of the F protein, leading to the virus-cell fusion and virus entry into the cell (6, 7). In addition, the expression of the H and F proteins on the cell surface causes the cell-cell fusion between infected and adjacent cells, producing multinucleated giant cells (syncytia).

The cellular receptors for MV are signaling lymphocyte activation

103 molecule (SLAM) expressed on immune cells (8, 9) and nectin 4 on epithelial
104 cells (10, 11). Since human neurons, an important target affected in SSPE,
105 express neither SLAM nor nectin 4 (12, 13), MV is thought to infect neurons
106 differently from non-neuronal target cells. Furthermore, free virus particles are
107 not usually detected in the brains of SSPE patients although viral RNA and
108 proteins are present (14-17). The Edmonston strain of MV (a
109 laboratory-adapted strain) can use ubiquitously expressed CD46 as an
110 additional receptor, through the mutations in the H gene (18, 19). It has been
111 shown that the Edmonston strain can infect and spread between primary
112 hippocampal neurons from CD46 transgenic mice that express human CD46 on
113 neurons (20). The transmission of the Edmonston strain between neurons was
114 blocked by the fusion inhibitor peptide (FIP) (21), and the virus could spread
115 from CD46+ to CD46- neurons in a cell-cell contact-dependent manner (20). The
116 authors proposed that only the F protein mediates the spread of MV between
117 neurons and that the H protein is dispensable for the process (21, 22). The
118 Edmonston strain was also shown to spread between rat hippocampal neurons
119 (23).

MVs recovered from brain tissues of SSPE patients (SSPE strains) contain characteristic features in their genomes. The function and expression of the M protein are impaired in most SSPE strains by such mechanisms as A-to-G hypermutations and read-through between the P and M genes (24-26). Because these mutations lead to the lower production of virus particles and possible evasion of the recognition by the host immune system, the defect of the M protein has been thought to contribute to neurovirulence (26, 27). The defective nature of the M protein also affects its ability to modulate viral RNA synthesis allowing enhanced transcription of the genome (28, 29). Furthermore, most SSPE strains have alterations in the cytoplasmic tail of the F protein (30, 31). Mutations causing the defect of the M protein or producing shortened cytoplasmic tails of the F and H proteins were shown to endow MV with hyperfusogenicity and facilitate MV spread in the brains of genetically modified mice (27).

More recent studies have shown that many SSPE strains possess amino acid substitutions in the extracellular domain of the F protein, which confer enhanced fusion activity in SLAM- or nectin 4-expressing cells (32, 33).

137 Importantly, recombinant MVs possessing these substitutions in the F protein,
138 but not the wild-type MV, cause syncytium formation even in SLAM- and nectin
139 4-negative cells including human neuroblastoma cell lines, and spread
140 efficiently in the brains of the type I interferon receptor subunit 1 (IFNAR1)
141 knockout mice and suckling hamsters as well as in human primary neurons (33,
142 34). The H protein of SSPE strains was also shown to be partly responsible for
143 neurovirulence (32, 35, 36).

144 In the present study, we aimed to examine how MV is transmitted
145 between neurons, by using cells and viruses relevant to MV infection in human
146 brains. To this end, we employed NTERA-2 cl. D1 (NT2), a human embryonal
147 carcinoma cell line, which can be differentiated into postmitotic neurons
148 following the treatment with retinoic acid (RA) (37-40). Removal of
149 undifferentiated cells by mitotic inhibitors increases the proportion of
150 differentiated neurons up to 95% (40). These cells express several
151 neurotransmitters (41), exhibit neuronal electrophysiological properties (42),
152 and have been used as human model neurons in the fields of basic sciences,
153 drug screening and clinical application (43). SSPE strains accumulate many

154 mutations during persistence, but generally do not have those in the H gene
155 that would allow them to utilize CD46 as a receptor (18, 44-46). Thus, we used
156 for this study the wild-type strain-based recombinant MV and its mutant
157 possessing an SSPE strain-derived substitution in the F protein.
158
159 ## Results
160 **Spread of the hyperfusogenic MV between NT2 neurons.** Enhanced green
161 fluorescent protein (EGFP)-expressing recombinant MVs possessing
162 fusion-enhancing substitutions in the F protein [e.g. IC323-F(T461I)-EGFP],
163 but not the parental MV possessing the wild-type F protein (IC323-EGFP),
164 efficiently spread in human primary neurons (34). To investigate mechanisms of
165 MV spread between human neurons in detail, we used human NT2 neurons
166 (NT2N), which are more tractable than primary neurons. Undifferentiated NT2
167 cells were differentiated into postmitotic neurons using the cell aggregate
168 method (40) (Fig. 1A). NT2N cells had small, phase-bright cell bodies and long
169 axons, and tended to form clusters, as previously reported (40). Expression
170 levels of several neuronal marker genes were greatly increased in NT2N cells

171 compared to undifferentiated cells (Fig. 1B). A small number of larger glia-like
172 cells were also present in the postmitotic cell population, but expression levels
173 of astrocytic marker genes were not elevated significantly compared to
174 undifferentiated cells (Fig. 1A, B).

175 To examine the effect of the fusion-enhancing substitution T461I in the
176 F protein on the spread of MV between neurons, NT2N cells were infected with
177 IC323-EGFP or IC323-F(T461I)-EGFP at a multiplicity of infection (MOI) of 2
178 (Fig. 2A). NT2N cells were also infected with VSVΔG*-G, which contains the
179 GFP gene in its genome and does not produce infectious particles because it
180 lacks the glycoprotein (G) gene (47), at an MOI of 0.05. Single infected cells were
181 observed one day after infection with any of the three viruses. At 2 days post
182 infection (d.p.i.), expression of EGFP was largely restricted to cells originally
183 infected with IC323-EGFP and hardly spread further. By contrast, expression of
184 EGFP spread efficiently from neurons infected with IC323-F(T461I)-EGFP to
185 adjacent cells, without syncytium formation (Fig. 2A). The spread of GFP
186 expression was never observed in VSVΔG*-G-infected neurons, indicating that
187 GFP per se cannot be transmitted between neurons. In addition, larger increase

188 in the expression of the MV-N protein was observed over time in neurons
189 infected with IC323-F(T461I)-EGFP, compared with those infected with
190 IC323-EGFP (Fig. 2B). Taken together, these results indicate that the
191 fusion-enhancing substitution in the F protein is critical for efficient spread of
192 MV in NT2N cells, and that the viral genome is indeed transmitted from
193 neurons infected with the hypefusogenic MV to adjacent neurons. After MV
194 infection, we continued to observe EGFP-positive infected NT2N cells, which
195 appeared to be damaged and died at 4-6 d.p.i. (data not shown).

196 **The hyperfusogenic MV spreads between NT2 neurons in a cell-to-cell**
197 **manner.** To examine how the hyperfusogenic MV spreads between NT2N cells,
198 we next performed a confocal time-lapse photography (Fig. 3A and Movie S1).
199 NT2N cells were infected with IC323-F(T461I)-EGFP, and observed under a
200 confocal microscope. At 24 h p.i., a small number of NT2N cells were
201 EGFP-positive. During observation, expression of EGFP efficiently spread from
202 originally infected neurons to those connected to them via axons, and the
203 number of EGFP-positive neurons increased over time.

204 IC323-F(T461I)-EGFP was reported to propagate in SLAM- or nectin

4-expressing cells at comparable levels with the wild-type MV until 48 h p.i (thereafter its titers decrease sharply due to strong cytopathic effects) (34). In contrast, it produced only low virus titers in NT2N cells for 4 days after infection (Fig. 3B), despite its efficient spread between the cells. The results, together with the above morphological findings, indicate that the hyperfusogenic virus spreads between NT2N cells mainly, if not exclusively, in a cell-to-cell manner.

Membrane fusion is involved in the spread of the hyperfusogenic MV between NT2N cells. While IC323-F(T461I)-EGFP induced syncytium formation in SLAM- and nectin 4-negative non-neuronal cells (e.g. Vero cells), it did not in human primary neurons and NT2N cells ((33, 34) and this study). However, it is possible that a small membrane fusion occurs between infected and adjacent cells, contributing to the spread of MV. To test this idea, we used FIP, which is known to inhibit membrane fusion induced by MV (48, 49). Vero cells expressing human SLAM (Vero/hSLAM) and NT2N cells were infected with IC323-F(T461I)-EGFP at an MOI of 0.1 for 1 h, and then incubated in the presence of FIP or the solvent dimethyl sulfoxide (DMSO). While Vero/hSLAM

222 cells treated with DMSO formed extensive syncytia at 1 d.p.i., FIP strongly
223 inhibited cell-cell fusion in them (Fig. 4). Remarkably, FIP completely blocked
224 the spread of IC323-F(T461I)-EGFP between NT2N cells, while DMSO had no
225 effect on the spread. The results suggest that membrane fusion is indeed
226 involved in the cell-to-cell spread of the hyperfusogenic MV between NT2N cells.
227 We also tested substance P, which was reported to inhibit membrane fusion
228 induced by MV (48, 49) and neuronal spread of the Edmonston strain (21).
229 Substance P inhibited neither syncytium formation in Vero/hSLAM cells nor the
230 spread of IC323-F(T461I)-EGFP between NT2N cells (data not shown).

231 **The H protein is required for the cell-to-cell spread of the**
232 **hyperfusogenic virus between NT2N cells.** To examine whether the H protein is
233 involved in MV spread between NT2N cells, we generated anti-H monoclonal
234 antibodies (MAbs) that can block SLAM- and nectin 4-dependent MV infection.
235 Vero/hSLAM cells and Vero cells expressing human nectin 4 (Vero/hNectin4)
236 were infected with IC323-EGFP, and NT2N cells with IC323-F(T461I)-EGFP at
237 an MOI of 0.1 for 1 h. The infected cells were then incubated in the presence of a
238 previously reported anti-H MAb 2F4 (50) or anti-H MAbs we generated (7C6,

8F6, and 10B5) and observed under a fluorescence microscope (Fig. 5A). The extents of syncytium formation or viral spread were also determined by quantitating EGFP-positive areas (Fig. 5B). All four MAbs examined inhibited, albeit to different extents, syncytium formation in IC323-EGFP-infected Vero/hSLAM and Vero/hNectin4 cells (Fig. 5A, B). When these cells were infected with the hyperfusogenic IC323-F(T461I)-EGFP, all the MAbs also exhibited inhibitory activity though to the lesser degree (data not shown). MAbs 2F4 and 8F6 were also able to inhibit the spread of IC323-F(T461I)-EGFP between NT2N cells, whereas 7C6 failed to do so (Fig. 5A, B). 10B5 exhibited a weaker ability to inhibit syncytium formation in Vero/hSLAM and Vero/hNectin4 cells than the other three MAbs, but it completely blocked the spread of IC323-F(T461I)-EGFP between NT2N cells (Fig. 5A, B).

Discussion

In this study, we demonstrated that the hyperfusogenic IC323-F(T461I)-EGFP, but not the parental wild-type IC323-EGFP, spread efficiently between human neuron NT2N cells. The finding is consistent with our previous results obtained

256 with this and other hyperfusogenic recombinant MVs in human primary neuron
257 culture and in the brains of suckling hamsters and IFNAR1 knockout mice (33,
258 34). Thus, enhanced fusion activity of the F protein appears to be essential for
259 efficient spread of MV in human and rodent neurons.

260 On the other hand, the Edmonston strain of MV has been shown to
261 spread between mouse (20) and rat neurons (23), without fusion-enhancing
262 substitutions in the F protein. The Edmonston strain has many substitutions in
263 the receptor-binding H protein including those allowing the use of CD46 as a
264 receptor (18, 19). However, CD46 is not critically involved in the spread of the
265 Edmonston strain because neurons from rats and CD46 non-transgenic mice do
266 not express CD46. At present there is no knowing whether the molecule
267 involved in the spread of the Edmonston strain between rodent neurons is the
268 same as the one used for MV spread between human neurons. Furthermore,
269 expression of CD46 on human neurons makes it difficult to interpret the results
270 obtained with the Edmonston strain. To avoid these problems and study what
271 indeed occurs in the human brain, we employed human neurons derived from
272 NT2 cells and wild-type MV-based recombinant viruses.

Because SLAM and nectin 4 are not expressed on human neurons, it is likely that MV uses other molecule(s) to enter and spread between neurons. Given that fusion-enhancing substitutions in the F protein strongly promote MV spread between human neurons, only the F protein, but not the H protein, may play a role in MV spread, as previously proposed (21, 22). However, most of anti-H MAbs (neutralizing infection via SLAM or nectin4) examined blocked the spread of IC323-F(T461I)-EGFP between NT2N cells. One MAb neutralized SLAM- and nectin 4-dependent MV infections, but did not inhibit the spread of IC323-F(T461I)-EGFP between NT2N cells. Another MAb only weakly inhibited syncytium formation in Vero/hSLAM and Vero/hNectin4 cells, but strongly blocked the spread of IC323-F(T461I)-EGFP between NT2N cells. These results suggest that the H protein is also required for the spread of the hyperfusogenic MV between NT2N cells, and that the region on the H protein involved in MV spread between neurons is overlapping with but different from that involved in the interaction with SLAM or nectin 4. Furthermore, these findings indicate the presence of the neuronal receptor interacting with the H protein of MV. In the sera and cerebrospinal fluids of SSPE patients, high levels of anti-MV Abs are

present (5). This means that MV can somehow escape from neutralization by these Abs in SSPE patients. Detailed analyses of amino acid substitutions in the H protein from SSPE strains may reveal the mechanisms by which MV spreads in the CNS in the presence of anti-H Abs.

In SSPE patients, MV persistently infects neurons without producing virus particles (14). The lack of virus production is attributed to the defect of the M protein (26, 27). Thus, it is thought that the cell-to-cell MV transmission occurs between neurons in the brains of SSPE patients. By using confocal time-lapse imaging, we observed the cell-to-cell spread of IC323-F(T461I)-EGFP between NT2N cells. The virus was found to spread from originally infected neurons to those connected to them via axons. Furthermore, little virus production was detected in NT2N cells, although IC323-F(T461I)-EGFP possesses the intact M gene unlike most SSPE strains. Similarly, the Edmonston strain (possessing the intact M protein) was reported to grow well in undifferentiated NT2 cells (presumably using CD46 as a receptor), but not in NT2 neurons (20). Thus, mutations in the M gene, a hallmark of SSPE strains, may partly result from the dispensability of the M protein for their survival in

neurons.

IC323-F(T461I)-EGFP did not induce syncytia in NT2N cells like in human primary neurons (34). However, its spread between NT2N cells was prevented by FIP, indicating that the cell-cell fusion does occur when the virus is transmitted. This is consistent with the clinical observation that syncytia are not present in the brains of SSPE patients (5). In the human brain, the cell-cell contacts between neurons may be hindered by other supporting cells and myelinated nerve fibers, and limited to small areas such as synapses. This spatial arrangement may be a reason why neurons do not form syncytia in SSPE patients. In our culture of NT2N cells, non-neuronal cells are very few, and the cell-cell contact appears to occur between cell bodies of different neurons. Thus, in NT2N cells, the membrane fusion may occur only at synapses where virus (RNP complex) transmission takes place between neurons, but may not occur in other parts of cells. Recently, it has been shown that peptides derived from the heptad repeat regions of the F protein can inhibit entry and cell fusion by MV, and protect model mice from MV-induced encephalitis (51-53). A fusion-enhancing substitution in the F protein was also found in MV genomes

from the brains of human immunodeficiency virus-infected patients with measles inclusion body encephalitis (54). Blocking of membrane fusion caused by mutant F proteins might be a good strategy to inhibit progression of fatal MV infection in the CNS.

In conclusion, the H protein and the mutant F protein possessing fusion-enhancing substitutions play crucial roles in membrane fusion and subsequent MV transmission between neurons. Our data also suggest that a molecule(s) other than SLAM and nectin 4 acts as a neuronal receptor for MV. We envisage that this putative receptor is highly concentrated at synapses.

Materials and Methods

Cells. Vero/hSLAM (9) and Vero/hNectin4 cells (55) were maintained in Dulbecco's modified Eagle's medium (DMEM; Wako Pure Chemical Industries) supplemented with 7.5% fetal bovine serum (FBS; Sigma) and 1% penicillin-streptomycin (Gibco). NTERA-2 cl. D1 (NT2) cells were purchased from American Type Culture Collection and maintained in Opti-MEM (Gibco) supplemented with 5% FBS and 1% penicillin-streptomycin. We slightly

341 modified the previously described protocol for neuronal differentiation of NT2
342 cells (40). Briefly, NT2 cells were suspended in DMEM supplemented with 10%
343 FBS, and seeded in bacteriological grade Petri dishes (Eiken Chemical) at a
344 density of 4–5 × 10^6 cells per dish. On the next day, all-trans RA (Sigma) was
345 added to culture medium at a final concentration of 10 μM. Every 2–3 days the
346 medium and dishes were changed. After 7–8 days, the cells were seeded in
347 10-cm cell culture dishes (Nippon Genetics) and cultured for another 6–8 days.
348 The cells were detached by trypsin (MP biomedicals), transferred to 15-cm cell
349 culture dishes (Nunc), and cultured without RA for 2 days. The cells were
350 trypsinized again, seeded in 10-cm cell culture dishes precoated with 10 μg of
351 poly-D-lysine (PDL; Sigma)/mL, 10 μg of laminin (LAM; Sigma)/mL and 0.1%
352 gelatin (Sigma), and supplied with medium containing a final concentration of
353 40 μM Cytosine ß-D-Arabinofuranoside (Ara-C; Sigma) and 4 μM Uridine
354 (Sigma). After 7–10 days, differentiated neurons (NT2N) were detached by brief
355 trypsinization and seeded in plates precoated with PDL, LAM, and gelatin for
356 further experiments.

357 **Viruses.** IC323-EGFP is a recombinant MV expressing EGFP based on

the wild-type IC-B strain (56, 57). IC323-F(T461I)-EGFP was generated, based on IC323-EGFP (33). The recombinant MVs were prepared as described (58) and titrated on Vero/hSLAM cells by plaque assay. VSVΔG*-G was prepared and titrated on 293T cells as previously described (47, 59).

Confocal time-lapse imaging. NT2N cells seeded in glass-bottom dishes (Matsunami Glass Ind.) were infected with IC323-F(T461I)-EGFP at an MOI of 2. EGFP fluorescence was observed under a confocal microscope (Radiance 2100; Bio-Rad). Images were taken every 15 min from 24 h p.i. to 40 h p.i.

Inhibition of virus spread by FIP. FIP (Z-D-Phe-Phe-Gly; Peptide institute) and substance P (H-Arg-Pro-Lys-Pro-Gln-Gln-Phe-Phe-Gly-Leu-Met-NH_2; Peptide institute) were dissolved in DMSO (Sigma). Vero/hSLAM and NT2N cells seeded in 24-well plates were infected with IC323-F(T461I)-EGFP at an MOI of 0.1. At 1 h p.i., DMSO, FIP, or substance P was added to the culture medium at a final concentration of 2% (DMSO) or 200 μM (FIP and substance P).

Inhibition of virus spread by anti-H MAbs. MAb 2F4 is a previously described antibody against MV-H (50). To generate anti-H MAbs, the expression

375 plasmid encoding soluble histidine (His)-tagged MV-H was transiently
376 transfected into HEK293S GnTI(-) cells (60, 61). One week after transfection,
377 culture medium containing the secreted MV-H was collected. MV-H was purified
378 by using the Ni^{2+}-NTA affinity column (cOmplete His-Tag Purification Resin;
379 Roche) and superdex 200 GL 10/300 gel filtration chromatography (GE
380 Healthcare). Six-week-old BALB/c mice were immunized with the purified
381 MV-H four times at intervals of 1 week. Three days after the last immunization,
382 the mice were euthanized, and spleen cells were harvested. All animal
383 experiments were reviewed by the Institutional Committee of Ethics on Animal
384 Experiments and carried out according to the Guidelines for Animal
385 Experiments of the Faculty of Medicine, Kyushu University, Japan. We
386 screened hybridoma cells for anti-H MAbs possessing neutralizing ability for
387 MV. Vero/hSLAM and Vero/hNectin4 cells were infected with IC323-EGFP
388 mixed with supernatants of hybridomas, and at 1 h p.i., FIP was added to the
389 culture medium. At 24-36 h p.i., EGFP fluorescence was observed under a
390 fluorescence microscope (Axiovert 200; Carl Zeiss). MV-neutralizing MAbs were
391 purified by protein G affinity chromatography. We verified by enzyme-linked

392 immunosorbent assay that all purified MV-neutralizing MAbs could bind to
393 MV-H. Vero/hSLAM, Vero/hNectin4 and NT2N cells were seeded in 96-well
394 plates and infected with IC323-EGFP or IC323-F(T461I)-EGFP at an MOI of 0.1.
395 At 1 h p.i., anti-H MAbs were added to the culture medium at a final
396 concentration of 10 μg/mL. Fluorescence images of cells were taken with
397 BZ-X710 (Keyence) at 48 h p.i. Relative areas of EGFP-expressing cells in
398 triplicate samples were determined using BZ-X Analyzer (Keyence).

399 **Reverse transcription-quantitative PCR (RT-qPCR).** RNA was extracted
400 with TRIzol (Invitrogen) from undifferentiated NT2 cells and postmitotic
401 neurons (NT2 cells treated with RA for 2 weeks and mitotic inhibitors for
402 another 1 week). The RNA samples were treated with RQ1 RNase-Free DNase
403 (Promega) and reverse transcribed using PrimeScript RT reagent Kit (Takara
404 Bio). Quantification of mRNAs of neuronal and astrocytic markers and
405 glyceraldehyde-3-phosphate dehydrogenase (GAPDH) was carried out using
406 SYBR Premix Ex Taq II (Takara Bio) and LightCycler 1.5 (Roche). For
407 microtubule-associated protein 2 (MAP2), microtubule-associated protein tau
408 (MAPT), RNA binding protein Fox-1 homolog 3 (RBFOX3), class III beta-tubulin

(TUBB3), glial fibrillary acidic protein (GFAP), and glutamate-ammonia ligase (GLUL), we used primer pairs 5'-TTTGGGCACACTCTTGTTGC-3' and 5'-TTGCTTCCGTTGGCATTTCG-3', 5'-CAGACCTGAAGAATGTCAAGTCC-3' and 5'-ACACTTGGAGGTCACCTTGC-3', 5'-GCAAATGTTCGGGCAATTCG-3' and 5'-ATCGTCCCATTCAGCTTCTCC-3', 5'-TCATCAGTGATGAGCATGGC-3' and 5'-TCGTTGTAGTAGACGCTGATCC-3', 5'-ACTCAATGCTGGCTTCAAGG-3' and 5'-AGCGAACCTTCTCGATGTAGC-3', and 5'-ATGCTGGAGTCAAGATTGCG-3' and 5'-AGTCTTCACACACACGATGC-3', respectively. Data were analyzed by a two-tailed Student's t test.

Western blotting. NT2N cells seeded in 12-well plates were infected with IC323-EGFP or IC323-F(T461I)-EGFP at an MOI of 2. The cells were washed by phosphate-buffered saline (PBS) and lysed in 1 × sodium dodecyl sulfate (SDS) loading buffer (40mM Tris HCl pH6.8, 1.6% SDS, 8% glycerol, 0.05% Bromophenol Blue, 0.1M dithiothreitol). Proteins in the lysate were separated by SDS-polyacrylamide gel electrophoresis (PAGE), and transferred to polyvinylidene difluoride membranes (Millipore). The membranes were blocked with PBS containing 0.05% Tween 20 and 5% skimmed milk, and subsequently

incubated with anti-MV serum for detection of MV-N (kindly provided by M. B. A. Oldstone) (62) or mouse anti-actin MAb (sc-8432; Santa Cruz Biotechnology). After washing with PBS-Tween 20 (PBS-T) three times, the membranes were incubated with goat anti-human IgG-horseradish peroxidase (HRP) or goat anti-mouse IgG-HRP (Jackson ImmunoResearch), washed by PBS-T three times again, and treated with Chemi-Lumi One Super (Nacalai Tesque). Chemiluminescent signals were detected by VersaDoc 5000 (Bio-Rad).

Acknowledgements

We thank M. B. A. Oldstone for providing the reagent. This study was supported by grants from the Ministry of Health, Labor and Welfare (the Research Committee of Prion Disease and Slow Virus Infection) of Japan (YY), by JSPS KAKENHI grant number 24115005 (YY), by AMED J-PRIDE grant number 17fm0208022h0001 (TH) and by GSK Japan Research grant 2017 (TH).

References

1. Griffin D. 2013. Measles virus, p 1042 – 1069. *In* Knipe D, Howley P, Cohen J, Griffin D, Lamb R, Martin M, Racaniello V, Roizman B (ed), Fields virology, 6th ed. Lippincott Williams & Wilkins, Philadelphia, PA.
2. Coughlin MM, Beck AS, Bankamp B, Rota PA. 2017. Perspective on Global Measles Epidemiology and Control and the Role of Novel Vaccination Strategies. Viruses 9:11.
3. Bellini WJ, Rota JS, Lowe LE, Katz RS, Dyken PR, Zaki SR, Shieh W-J, Rota PA. 2005. Subacute Sclerosing Panencephalitis: More Cases of This Fatal Disease Are Prevented by Measles Immunization than Was Previously Recognized. The Journal of Infectious Diseases 192:1686-1693.
4. Schönberger K, Ludwig M-S, Wildner M, Weissbrich B. 2013. Epidemiology of Subacute Sclerosing Panencephalitis (SSPE) in Germany from 2003 to 2009: A Risk Estimation. PLOS ONE 8:e68909.
5. Gutierrez J, Issacson RS, Koppel BS. 2010. Subacute sclerosing panencephalitis: an update. Dev Med Child Neurol 52:901-7.
6. Hashiguchi T, Ose T, Kubota M, Maita N, Kamishikiryo J, Maenaka K, Yanagi Y. 2011. Structure of the measles virus hemagglutinin bound to its cellular receptor SLAM. Nat Struct Mol Biol 18:135-41.
7. Plattet P, Alves L, Herren M, Aguilar H. 2016. Measles Virus Fusion Protein: Structure, Function and Inhibition. Viruses 8:112.
8. Tatsuo H, Ono N, Tanaka K, Yanagi Y. 2000. SLAM (CDw150) is a cellular receptor for measles virus. Nature 406:893-7.
9. Ono N, Tatsuo H, Hidaka Y, Aoki T, Minagawa H, Yanagi Y. 2001. Measles Viruses on Throat Swabs from Measles Patients Use Signaling Lymphocytic Activation Molecule (CDw150) but Not CD46 as a Cellular Receptor. Journal of Virology 75:4399-4401.
10. Noyce RS, Bondre DG, Ha MN, Lin LT, Sisson G, Tsao MS, Richardson CD. 2011. Tumor cell marker PVRL4 (nectin 4) is an epithelial cell receptor for measles virus. PLoS Pathog 7:e1002240.
11. Muhlebach MD, Mateo M, Sinn PL, Prufer S, Uhlig KM, Leonard VHJ, Navaratnarajah CK, Frenzke M, Wong XX, Sawatsky B, Ramachandran S, McCray PB, Cichutek K, von Messling V, Lopez M, Cattaneo R. 2011. Adherens junction protein nectin-4 is the epithelial receptor for measles virus. Nature 480:530-533.

12. McQuaid S, Cosby SL. 2002. An Immunohistochemical Study of the Distribution of the Measles Virus Receptors, CD46 and SLAM, in Normal Human Tissues and Subacute Sclerosing Panencephalitis. Lab Invest 82:403-409.
13. Reymond N, Fabre S, Lecocq E, Adelaïde J, Dubreuil P, Lopez M. 2001. Nectin4/PRR4, a New Afadin-associated Member of the Nectin Family That Trans-interacts with Nectin1/PRR1 through V Domain Interaction. Journal of Biological Chemistry 276:43205-43215.
14. Paula-Barbosa MM, Cruz C. 1981. Nerve cell fusion in a case of subacute sclerosing panencephalitis. Ann Neurol 9:400-3.
15. Lewandowska E, Lechowicz W, Szpak GM, Sobczyk W. 2001. Quantitative evaluation of intranuclear inclusions in SSPE: correlation with disease duration. Folia Neuropathol 39:237-41.
16. Godec MS, Asher DM, Swoveland PT, Eldadah ZA, Feinstone SM, Goldfarb LG, Gibbs CJ, Jr., Gajdusek DC. 1990. Detection of measles virus genomic sequences in SSPE brain tissue by the polymerase chain reaction. J Med Virol 30:237-44.
17. Kühne Simmonds M, Brown DWG, Jin L. 2006. Measles viral load may reflect SSPE disease progression. Virology Journal 3:49.
18. Lecouturier V, Fayolle J, Caballero M, Carabana J, Celma ML, Fernandez-Munoz R, Wild TF, Buckland R. 1996. Identification of two amino acids in the hemagglutinin glycoprotein of measles virus (MV) that govern hemadsorption, HeLa cell fusion, and CD46 downregulation: phenotypic markers that differentiate vaccine and wild-type MV strains. J Virol 70:4200-4.
19. Tahara M, Takeda M, Seki F, Hashiguchi T, Yanagi Y. 2007. Multiple Amino Acid Substitutions in Hemagglutinin Are Necessary for Wild-Type Measles Virus To Acquire the Ability To Use Receptor CD46 Efficiently. Journal of Virology 81:2564-2572.
20. Lawrence DM, Patterson CE, Gales TL, D'Orazio JL, Vaughn MM, Rall GF. 2000. Measles virus spread between neurons requires cell contact but not CD46 expression, syncytium formation, or extracellular virus production. J Virol 74:1908-18.
21. Makhortova NR, Askovich P, Patterson CE, Gechman LA, Gerard NP, Rall GF. 2007. Neurokinin-1 enables measles virus trans-synaptic spread in neurons. Virology 362:235-244.
22. Young VA, Rall GF. 2009. Making it to the synapse: Measles virus spread in and among neurons. Current topics in microbiology and immunology 330:3-30.

508 23. Ehrengruber MU, Ehler E, Billeter MA, Naim HY. 2002. Measles Virus Spreads in Rat
509 Hippocampal Neurons by Cell-to-Cell Contact and in a Polarized Fashion. Journal of
510 Virology 76:5720-5728.
511 24. Cattaneo R, Schmid A, Rebmann G, Baczko K, Ter Meulen V, Bellini WJ, Rozenblatt S,
512 Billeter MA. 1986. Accumulated measles virus mutations in a case of subacute
513 sclerosing panencephalitis: interrupted matrix protein reading frame and transcription
514 alteration. Virology 154:97-107.
515 25. Ayata M, Komase K, Shingai M, Matsunaga I, Katayama Y, Ogura H. 2002. Mutations
516 Affecting Transcriptional Termination in the P Gene End of Subacute Sclerosing
517 Panencephalitis Viruses. Journal of Virology 76:13062-13068.
518 26. Patterson JB, Cornu TI, Redwine J, Dales S, Lewicki H, Holz A, Thomas D, Billeter MA,
519 Oldstone MB. 2001. Evidence that the hypermutated M protein of a subacute sclerosing
520 panencephalitis measles virus actively contributes to the chronic progressive CNS
521 disease. Virology 291:215-25.
522 27. Cathomen T, Mrkic B, Spehner D, Drillien R, Naef R, Pavlovic J, Aguzzi A, Billeter MA,
523 Cattaneo R. 1998. A matrix-less measles virus is infectious and elicits extensive cell
524 fusion: consequences for propagation in the brain. The EMBO Journal 17:3899-3908.
525 28. Suryanarayana K, Baczko K, ter Meulen V, Wagner RR. 1994. Transcription inhibition
526 and other properties of matrix proteins expressed by M genes cloned from measles
527 viruses and diseased human brain tissue. J Virol 68:1532-43.
528 29. Reuter T, Weissbrich B, Schneider-Schaulies S, Schneider-Schaulies J. 2006. RNA
529 interference with measles virus N, P, and L mRNAs efficiently prevents and with matrix
530 protein mRNA enhances viral transcription. J Virol 80:5951-7.
531 30. Cattaneo R, Schmid A, Eschle D, Baczko K, ter Meulen V, Billeter MA. 1988. Biased
532 hypermutation and other genetic changes in defective measles viruses in human brain
533 infections. Cell 55:255-65.
534 31. Schmid A, Spielhofer P, Cattaneo R, Baczko K, ter Meulen V, Billeter MA. 1992.
535 Subacute sclerosing panencephalitis is typically characterized by alterations in the
536 fusion protein cytoplasmic domain of the persisting measles virus. Virology 188:910-5.
537 32. Ayata M, Takeuchi K, Takeda M, Ohgimoto S, Kato S, Sharma LB, Tanaka M,
538 Kuwamura M, Ishida H, Ogura H. 2010. The F Gene of the Osaka-2 Strain of Measles
539 Virus Derived from a Case of Subacute Sclerosing Panencephalitis Is a Major
540 Determinant of Neurovirulence. Journal of Virology 84:11189-11199.

33. Watanabe S, Shirogane Y, Suzuki SO, Ikegame S, Koga R, Yanagi Y. 2013. Mutant fusion proteins with enhanced fusion activity promote measles virus spread in human neuronal cells and brains of suckling hamsters. J Virol 87:2648-59.
34. Watanabe S, Ohno S, Shirogane Y, Suzuki SO, Koga R, Yanagi Y. 2015. Measles Virus Mutants Possessing the Fusion Protein with Enhanced Fusion Activity Spread Effectively in Neuronal Cells, but Not in Other Cells, without Causing Strong Cytopathology. Journal of Virology 89:2710-2717.
35. Cattaneo R, Rose JK. 1993. Cell fusion by the envelope glycoproteins of persistent measles viruses which caused lethal human brain disease. Journal of Virology 67:1493-1502.
36. Honda T, Yoneda M, Sato H, Kai C. 2013. Pathogenesis of Encephalitis Caused by Persistent Measles Virus Infection, p Ch. 14. *In* Tkachev S (ed), Encephalitis. InTech, Rijeka.
37. Andrews PW. 1984. Retinoic acid induces neuronal differentiation of a cloned human embryonal carcinoma cell line in vitro. Developmental Biology 103:285-293.
38. Pleasure SJ, Page C, Lee VM. 1992. Pure, postmitotic, polarized human neurons derived from NTera 2 cells provide a system for expressing exogenous proteins in terminally differentiated neurons. J Neurosci 12:1802-15.
39. Cheung WM, Fu WY, Hui WS, Ip NY. 1999. Production of human CNS neurons from embryonal carcinoma cells using a cell aggregation method. Biotechniques 26:946-8, 950-2, 954.
40. Paquet-Durand F, Tan S, Bicker G. 2003. Turning teratocarcinoma cells into neurons: rapid differentiation of NT-2 cells in floating spheres. Developmental Brain Research 142:161-167.
41. Podrygajlo G, Tegenge MA, Gierse A, Paquet-Durand F, Tan S, Bicker G, Stern M. 2009. Cellular phenotypes of human model neurons (NT2) after differentiation in aggregate culture. Cell Tissue Res 336:439-52.
42. Podrygajlo G, Song Y, Schlesinger F, Krampfl K, Bicker G. 2010. Synaptic currents and transmitter responses in human NT2 neurons differentiated in aggregate culture. Neuroscience Letters 468:207-210.
43. Paquet-Durand F, Bicker G. 2007. Human model neurons in studies of brain cell damage and neural repair. Curr Mol Med 7:541-54.
44. Rima BK, Earle JA, Baczko K, ter Meulen V, Liebert UG, Carstens C, Carabana J,

574 Caballero M, Celma ML, Fernandez-Munoz R. 1997. Sequence divergence of measles
575 virus haemagglutinin during natural evolution and adaptation to cell culture. J Gen
576 Virol 78 (Pt 1):97-106.
577 45. Shingai M, Ayata M, Ishida H, Matsunaga I, Katayama Y, Seya T, Tatsuo H, Yanagi Y,
578 Ogura H. 2003. Receptor use by vesicular stomatitis virus pseudotypes with
579 glycoproteins of defective variants of measles virus isolated from brains of patients with
580 subacute sclerosing panencephalitis. J Gen Virol 84:2133-43.
581 46. Hotta H, Nihei K, Abe Y, Kato S, Jiang DP, Nagano-Fujii M, Sada K. 2006. Full-length
582 sequence analysis of subacute sclerosing panencephalitis (SSPE) virus, a mutant of
583 measles virus, isolated from brain tissues of a patient shortly after onset of SSPE.
584 Microbiol Immunol 50:525-34.
585 47. Takada A, Robison C, Goto H, Sanchez A, Murti KG, Whitt MA, Kawaoka Y. 1997. A
586 system for functional analysis of Ebola virus glycoprotein. Proc Natl Acad Sci U S A
587 94:14764-9.
588 48. Richardson CD, Scheid A, Choppin PW. 1980. Specific inhibition of paramyxovirus and
589 myxovirus replication by oligopeptides with amino acid sequences similar to those at the
590 N-termini of the Fl or HA2 viral polypeptides. Virology 105:205-222.
591 49. Harrowe G, Mitsuhashi M, Payan DG. 1990. Measles virus-substance P receptor
592 interactions. Possible novel mechanism of viral fusion. J Clin Invest 85:1324-7.
593 50. Tahara M, Ohno S, Sakai K, Ito Y, Fukuhara H, Komase K, Brindley MA, Rota PA,
594 Plemper RK, Maenaka K, Takeda M. 2013. The Receptor-Binding Site of the Measles
595 Virus Hemagglutinin Protein Itself Constitutes a Conserved Neutralizing Epitope.
596 Journal of Virology 87:3583-3586.
597 51. Welsch JC, Talekar A, Mathieu C, Pessi A, Moscona A, Horvat B, Porotto M. 2013. Fatal
598 Measles Virus Infection Prevented by Brain-Penetrant Fusion Inhibitors. Journal of
599 Virology 87:13785-13794.
600 52. Mathieu C, Huey D, Jurgens E, Welsch JC, DeVito I, Talekar A, Horvat B, Niewiesk S,
601 Moscona A, Porotto M. 2015. Prevention of measles virus infection by intranasal
602 delivery of fusion inhibitor peptides. J Virol 89:1143-55.
603 53. Figueira TN, Palermo LM, Veiga AS, Huey D, Alabi CA, Santos NC, Welsch JC, Mathieu
604 C, Horvat B, Niewiesk S, Moscona A, Castanho MA, Porotto M. 2017. In Vivo Efficacy of
605 Measles Virus Fusion Protein-Derived Peptides Is Modulated by the Properties of
606 Self-Assembly and Membrane Residence. J Virol 91.

607 54. Jurgens EM, Mathieu C, Palermo LM, Hardie D, Horvat B, Moscona A, Porotto M. 2015.
608 Measles Fusion Machinery Is Dysregulated in Neuropathogenic Variants. mBio 6.
609 55. Otsuki N, Sekizuka T, Seki F, Sakai K, Kubota T, Nakatsu Y, Chen S, Fukuhara H,
610 Maenaka K, Yamaguchi R, Kuroda M, Takeda M. 2013. Canine distemper virus with the
611 intact C protein has the potential to replicate in human epithelial cells by using human
612 nectin4 as a receptor. Virology 435:485-492.
613 56. Takeda M, Takeuchi K, Miyajima N, Kobune F, Ami Y, Nagata N, Suzaki Y, Nagai Y,
614 Tashiro M. 2000. Recovery of Pathogenic Measles Virus from Cloned cDNA. Journal of
615 Virology 74:6643-6647.
616 57. Hashimoto K, Ono N, Tatsuo H, Minagawa H, Takeda M, Takeuchi K, Yanagi Y. 2002.
617 SLAM (CD150)-Independent Measles Virus Entry as Revealed by Recombinant Virus
618 Expressing Green Fluorescent Protein. Journal of Virology 76:6743-6749.
619 58. Seki F, Yamada K, Nakatsu Y, Okamura K, Yanagi Y, Nakayama T, Komase K, Takeda
620 M. 2011. The SI Strain of Measles Virus Derived from a Patient with Subacute
621 Sclerosing Panencephalitis Possesses Typical Genome Alterations and Unique Amino
622 Acid Changes That Modulate Receptor Specificity and Reduce Membrane Fusion
623 Activity. Journal of Virology 85:11871-11882.
624 59. Tatsuo H, Okuma K, Tanaka K, Ono N, Minagawa H, Takade A, Matsuura Y, Yanagi Y.
625 2000. Virus Entry Is a Major Determinant of Cell Tropism of Edmonston and Wild-Type
626 Strains of Measles Virus as Revealed by Vesicular Stomatitis Virus Pseudotypes
627 Bearing Their Envelope Proteins. Journal of Virology 74:4139-4145.
628 60. Reeves PJ, Callewaert N, Contreras R, Khorana HG. 2002. Structure and function in
629 rhodopsin: high-level expression of rhodopsin with restricted and homogeneous
630 N-glycosylation by a tetracycline-inducible N-acetylglucosaminyltransferase I-negative
631 HEK293S stable mammalian cell line. Proc Natl Acad Sci U S A 99:13419-24.
632 61. Hashiguchi T, Kajikawa M, Maita N, Takeda M, Kuroki K, Sasaki K, Kohda D, Yanagi Y,
633 Maenaka K. 2007. Crystal structure of measles virus hemagglutinin provides insight
634 into effective vaccines. Proc Natl Acad Sci U S A 104:19535-40.
635 62. Yanagi Y, Cubitt BA, Oldstone MBA. 1992. Measles virus inhibits mitogen-induced T
636 cell proliferation but does not directly perturb the T cell activation process inside the
637 cell. Virology 187:280-289.

638

Figure Legends

Figure 1. Neuronal differentiation of NT2 cells. (A) Phase-contrast images of undifferentiated NT2 cells and postmitotic NT2 neurons (NT2N). For neuronal differentiation, NT2 cells were treated with RA for 2 weeks, and mitotic inhibitors for additional 1 week. NT2 neurons tended to form clusters (arrow). There were a small number of glia-like cells in the postmitotic cell population (arrowhead). Scale bar, 250 μm. **(B)** Relative gene expression levels of neuronal (MAP2, MAPT, RBFOX3, and TUBB3) and astrocytic (GFAP and GLUL) markers in NT2 and NT2N cells were quantified by RT-qPCR. Data were normalized to those of GAPDH and presented as mean ± standard error of the mean (SEM) of three independent experiments. Asterisks indicate statistically significant increases compared with NT2 ($P < 0.05$).

Figure 2. Spread of recombinant MVs in NT2N cells. (A) NT2N cells were infected with IC323-EGFP or IC323-F(T461I)-EGFP at an MOI of 2. NT2N cells were also infected with VSVΔG*-G at an MOI of 0.05. The cells were observed under a light and a fluorescence microscope at 1 and 2 d.p.i. Representative

656 images are shown. The same areas were photographed each day. Arrowheads
657 indicate the same infected cell in IC323-EGFP- or VSVΔG*-G-infected NT2N
658 cells, respectively. Scale bar, 250 μm. **(B)** NT2N cells were infected with
659 IC323-EGFP or IC323-F(T461I)-EGFP at an MOI of 2, and cell lysates were
660 collected at the indicated time points. The samples were subjected to
661 SDS-PAGE and Western blotting using an antibody against the N protein
662 (MV-N). Actin was used as a loading control. Relative expression levels of the N
663 protein normalized to that of actin are indicated for each time point. The value
664 of 3 h p.i. was set to 1 for each virus. (-), uninfected.
665
666 **Figure 3. Cell-to-cell spread of the hyperfusogenic virus in NT2N cells. (A)**
667 NT2N cells were infected with IC323-F(T461I)-EGFP at an MOI of 2, and
668 observed by confocal time-lapse imaging. Arrowheads indicate the spread of
669 EGFP expression from an infected neuron to an adjacent cell. See also Movie S1
670 in the supplemental material. **(B)** Growth kinetics of IC323-F(T461I)-EGFP in
671 NT2N cells. NT2N cells were infected as in (A). Supernatants and cells were
672 harvested at 3, 24, 48, 72, and 96 h p.i. Virus titer (combined titer of

673 cell-associated and cell-free viruses) at each time point was determined by
674 plaque assay. Data are shown as mean ± standard deviation (SD) of triplicate
675 samples. The dotted line depicts the detection limit.
676
677 **Figure 4. Spread of the hyperfusogenic virus is inhibited by FIP.** Vero/hSLAM
678 and NT2N cells were infected with IC323-F(T461I)-EGFP at an MOI of 0.1. At 1
679 h p.i., FIP or the solvent DMSO was added to the culture medium at a final
680 concentration of 200 μM. The cells were observed under a light and a
681 fluorescence microscope at the indicated day after infection. The panels show
682 representative images. Scale bar, 250 μm.
683
684 **Figure 5. Spread of the hyperfusogenic virus is inhibited by anti-hemagglutinin**
685 **antibodies.** Cells were seeded in 96-well plates. Vero/hSLAM and Vero/hNectin4
686 cells were infected with IC323-EGFP and NT2N cells with
687 IC323-F(T461I)-EGFP at an MOI of 0.1 in triplicate. At 1 h p.i., the indicated
688 MAbs against the MV-H protein were added to the culture medium. As a
689 negative control, anti-H MAb 5G7, which has no ability to neutralize MV, was

690 used. EGFP fluorescence was observed under a fluorescence microscope at 48 h
691 p.i. **(A)** Fluorescence image of a representative well is shown for each sample.
692 Ab(-), no antibody. **(B)** Relative areas of EGFP-expressing cells in each well were
693 quantified by imaging software. Data are shown as mean ± SD of triplicate
694 samples. The value of Ab(-) was set to 1 for each cell type.

Figure 1

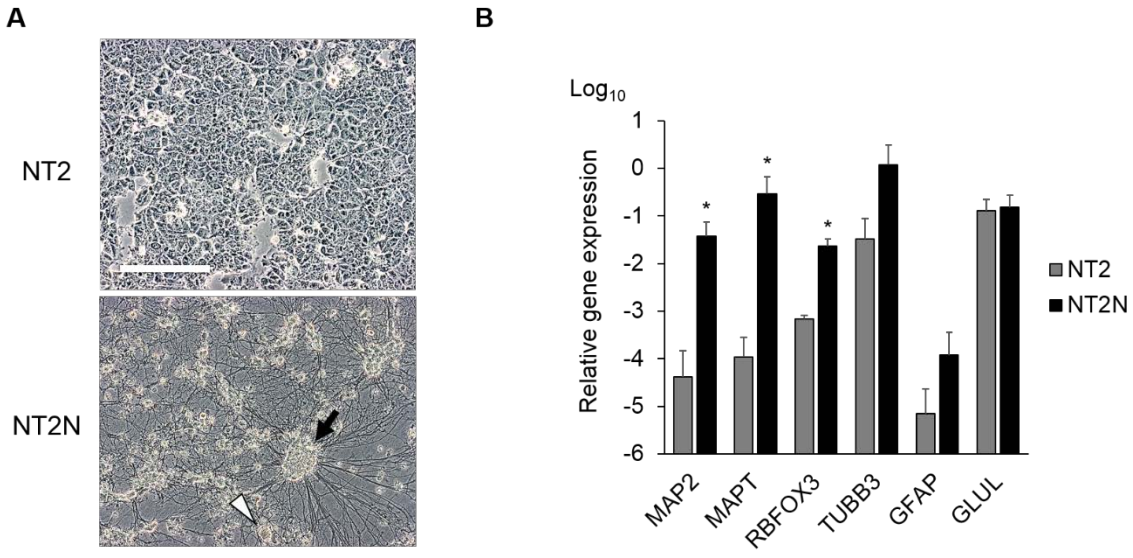

Figure 1. Neuronal differentiation of NT2 cells. (A) Phase-contrast images of undifferentiated NT2 cells and postmitotic NT2 neurons (NT2N). For neuronal differentiation, NT2 cells were treated with RA for 2 weeks, and mitotic inhibitors for additional 1 week. NT2 neurons tended to form clusters (arrow). There were a small number of glia-like cells in the postmitotic cell population (arrowhead). Scale bar, 250 μm. (B) Relative gene expression levels of neuronal (MAP2, MAPT, RBFOX3, and TUBB3) and astrocytic (GFAP and GLUL) markers in NT2 and NT2N cells were quantified by RT-qPCR. Data were normalized to those of GAPDH and presented as mean ± standard error of the mean (SEM) of three independent experiments. Asterisks indicate statistically significant increases compared with NT2 ($P < 0.05$).

Figure 2

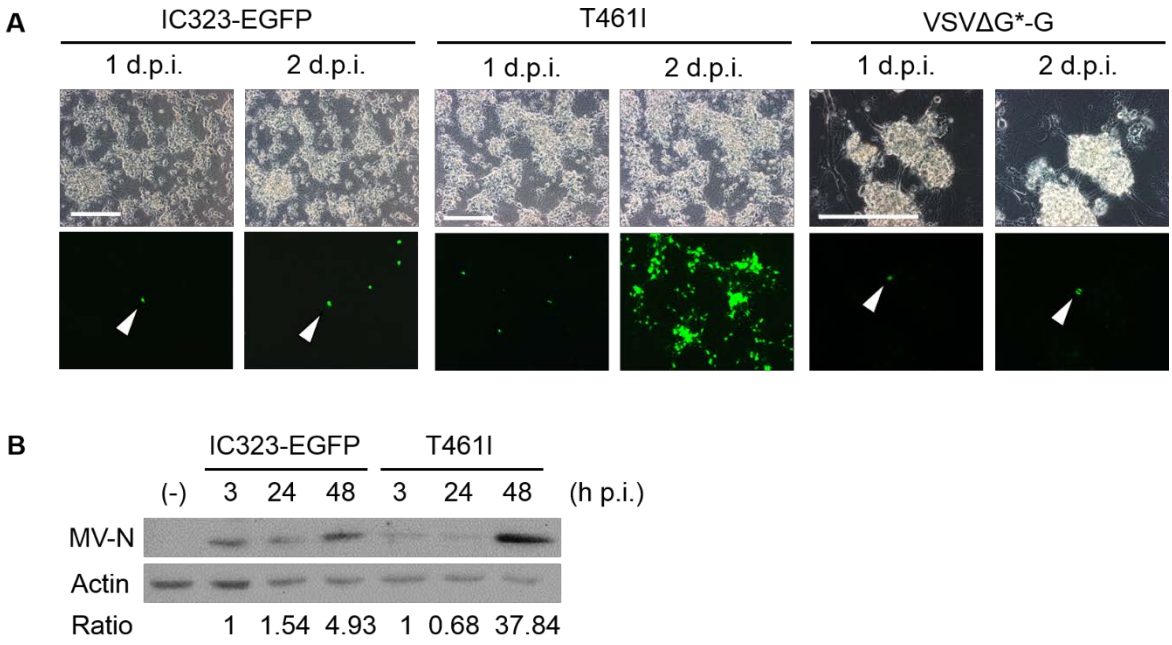

Figure 2. Spread of recombinant MVs in NT2N cells. (A) NT2N cells were infected with IC323-EGFP or IC323-F(T461I)-EGFP at an MOI of 2. NT2N cells were also infected with VSVΔG*-G at an MOI of 0.05. The cells were observed under a light and a fluorescence microscope at 1 and 2 d.p.i. Representative images are shown. The same areas were photographed each day. Arrowheads indicate the same infected cell in IC323-EGFP- or VSVΔG*-G-infected NT2N cells, respectively. Scale bar, 250 µm. (B) NT2N cells were infected with IC323-EGFP or IC323-F(T461I)-EGFP at an MOI of 2, and cell lysates were collected at the indicated time points. The samples were subjected to SDS-PAGE and Western blotting using an antibody against the N protein (MV-N). Actin was used as a loading control. Relative expression levels of the N protein normalized to that of actin are indicated for each time point. The value of 3 h p.i. was set to 1 for each virus. (-), uninfected.

Figure 3

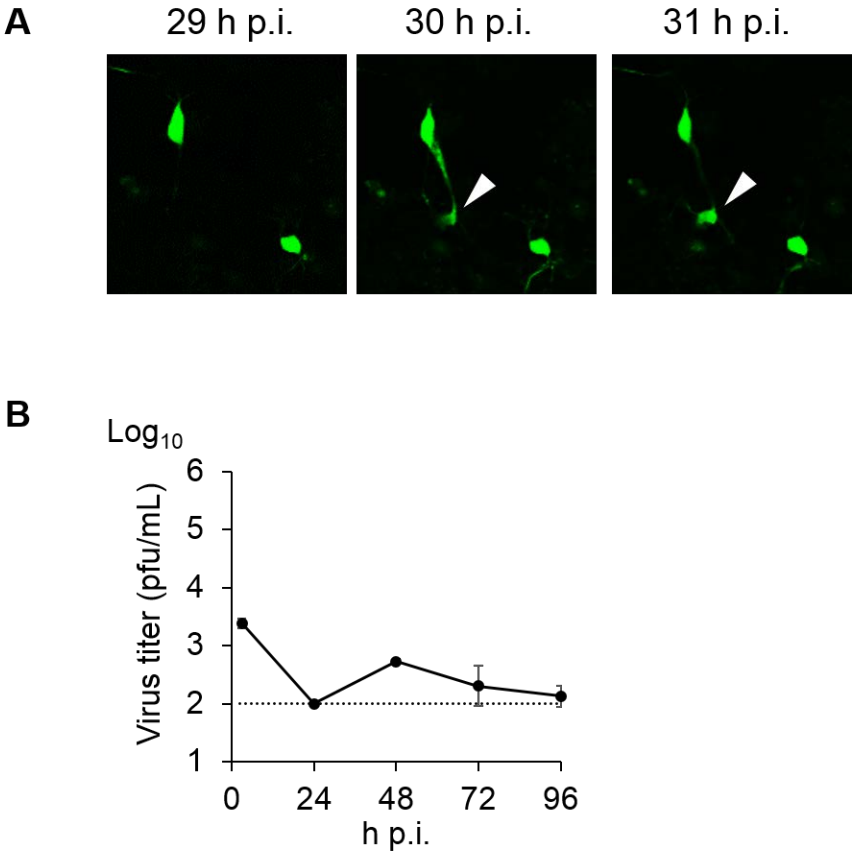

Figure 3. Cell-to-cell spread of the hyperfusogenic virus in NT2N cells. (A) NT2N cells were infected with IC323-F(T461I)-EGFP at an MOI of 2, and observed by confocal time-lapse imaging. Arrowheads indicate the spread of EGFP expression from an infected neuron to an adjacent cell. See also Movie S1 in the supplemental material. (B) Growth kinetics of IC323-F(T461I)-EGFP in NT2N cells. NT2N cells were infected as in (A). Supernatants and cells were harvested at 3, 24, 48, 72, and 96 h p.i. Virus titer (combined titer of cell-associated and cell-free viruses) at each time point was determined by plaque assay. Data are shown as mean ± standard deviation (SD) of triplicate samples. The dotted line depicts the detection limit.

Figure 4

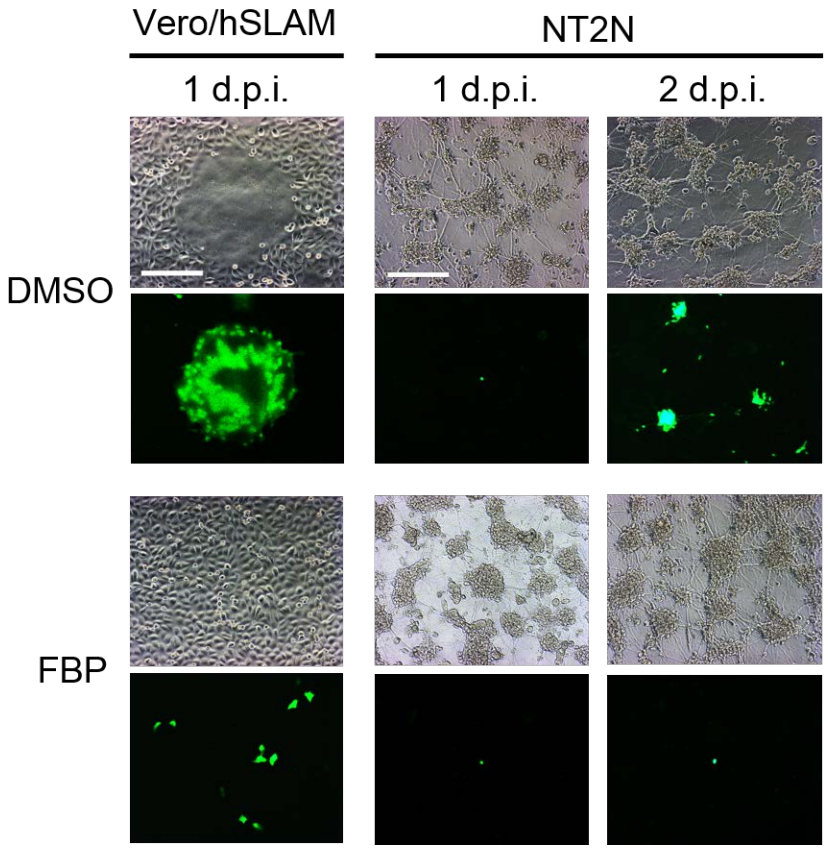

Figure 4. Spread of the hyperfusogenic virus is inhibited by FIP. Vero/hSLAM and NT2N cells were infected with IC323-F(T461I)-EGFP at an MOI of 0.1. At 1 h p.i., FIP or the solvent DMSO was added to the culture medium at a final concentration of 200 μM. The cells were observed under a light and a fluorescence microscope at the indicated day after infection. The panels show representative images. Scale bar, 250 μm.

Figure 5

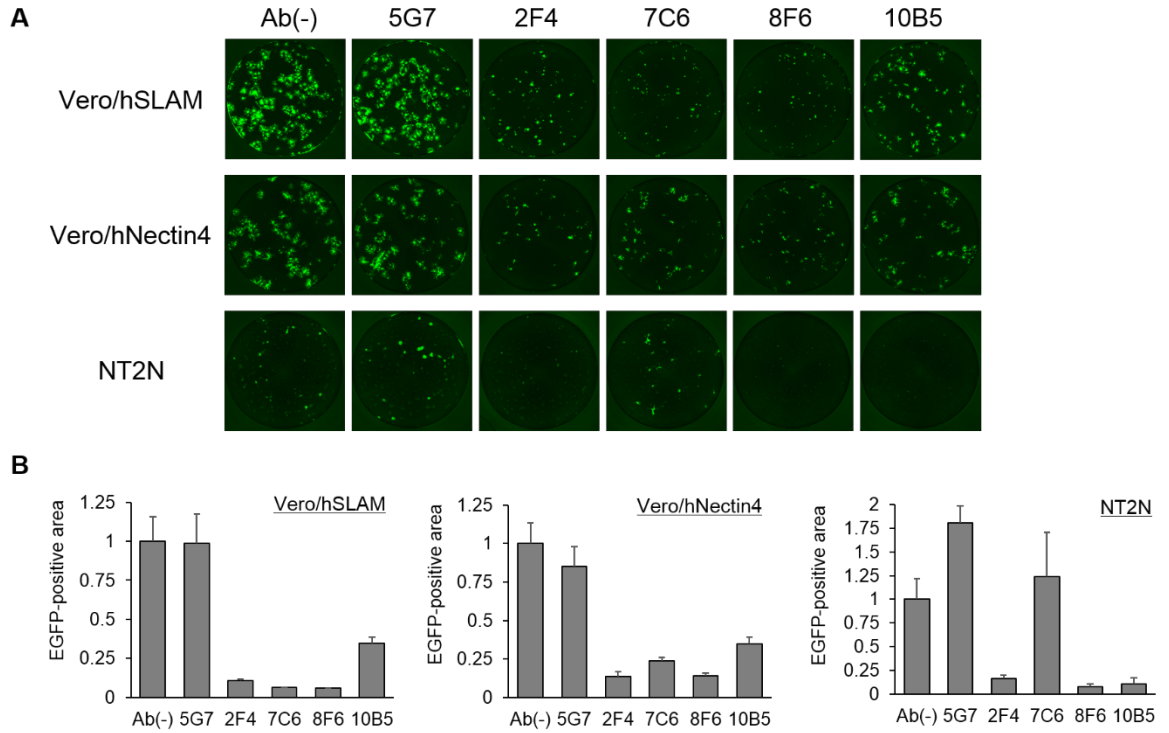

Figure 5. Spread of the hyperfusogenic virus is inhibited by anti-hemagglutinin antibodies. Cells were seeded in 96-well plates. Vero/hSLAM and Vero/hNectin4 cells were infected with IC323-EGFP and NT2N cells with IC323-F(T461I)-EGFP at an MOI of 0.1 in triplicate. At 1 h p.i., the indicated MAbs against the MV-H protein were added to the culture medium. As a negative control, anti-H MAb 5G7, which has no ability to neutralize MV, was used. EGFP fluorescence was observed under a fluorescence microscope at 48 h p.i. (A) Fluorescence image of a representative well is shown for each sample. Ab(-), no antibody. (B) Relative areas of EGFP-expressing cells in each well were quantified by imaging software. Data are shown as mean ± SD of triplicate samples. The value of Ab(-) was set to 1 for each cell type.